DOI: 10.6060/ivkkt.20246711.7073

УДК: 537.525

О ВЛИЯНИИ ИНЕРТНОГО ГАЗА-НОСИТЕЛЯ НА КОНЦЕНТРАЦИИ АКТИВНЫХ ЧАСТИЦ И КИНЕТИКУ ТРАВЛЕНИЯ ZrO_2 В ПЛАЗМЕ ХЛОРА

А.М. Ефремов, С.А. Смирнов, В.Б. Бетелин, К.-Н. Kwon

Александр Михайлович Ефремов (ORCID 0000-0002-9125-0763) *

НИИМЭ, ул. Академика Валиева, 6/1, Зеленоград, Москва, Российская Федерация, 124460
E-mail: amefremov@mail.ru*

Сергей Александрович Смирнов (ORCID 0000-0002-0375-0494)

Ивановский государственный химико-технологический университет, Шереметевский пр., 7, Иваново, Российская Федерация, 153000
E-mail: sas@isuct.ru

Владимир Борисович Бетелин (ORCID 0000-0001-6646-2660)

ФГУ ФНЦ НИИСИ РАН, Нахимовский пр., 36, к.1, Москва, Российская Федерация, 117218
E-mail: betelin@niisi.msk.ru

Kwang-Ho Kwon (ORCID 0000-0003-2580-8842)

Korea University, 208 Seochang-Dong, Chochiwon, Korea, 339-800
E-mail: kwonkh@korea.ac.kr

Исследовано влияние вида и содержания инертного газа-носителя на электрофизические параметры плазмы хлора, стационарные концентрации активных частиц и кинетику их взаимодействия с ZrO_2 в условиях "мягкого" реактивно-ионного травления. Данный режим предполагает использование более низкого, чем обычно, отрицательного смещения для снижения энергии ионной бомбардировки и дефектообразования на обрабатываемой поверхности. При совместном использовании диагностики плазмы с помощью зондов Ленгмюра и 0-мерного моделирования плазмы проведен анализ кинетики процессов образования и гибели активных частиц в смесях переменного начального состава. Найдено, что добавка к хлору Ar или He при постоянном общем давлении смеси а) способствует увеличению температуры и концентрации электронов; б) вызывает рост степени диссоциации молекул Cl_2 за счет ускорения процессов под действием электронного удара; и в) интенсифицирует ионную бомбардировку за счет изменения плотности потока ионов. Эксперименты показали, что скорость травления ZrO_2 определяется, в основном, химической составляющей, но не коррелирует с изменением плотности потока атомов хлора. Такая ситуация означает, что а) доминирующим механизмом травления ZrO_2 является ионно-стимулированная химическая реакция и б) увеличение эффективной вероятности этой реакции в смесях с высоким содержанием Ar или He отражает ускорение ионно-индуцированных гетерогенных эффектов, таких как разрушение связей Zr-O и/или десорбция слаболетучих соединений $ZrCl_x$. Более низкое отношение плотностей потоков нейтральных и заряженных частиц, наблюдаемое при разбавлении хлора аргоном, позволяет предположить более анизотропное травление. Показано, что отмеченные особенности уверенно сохраняются в диапазоне давлений 4–12 мтор и мощностей смещения 100–300 Вт.

Ключевые слова: Cl_2, Ar, плазма, параметры, активные частицы, ионизация, диссоциация, травление, вероятность реакции

Для цитирования:
Ефремов А.М., Смирнов С.А., Бетелин В.Б., Kwon K.-H. О влиянии инертного газа-носителя на концентрации активных частиц и кинетику травления ZrO_2 в плазме хлора. *Изв. вузов. Химия и хим. технология*. 2024. Т. 67. Вып. 11. С. 40–54. DOI: 10.6060/ivkkt.20246711.7073.

For citation:
Efremov A.M., Smirnov S.A., Betelin V.B., Kwon K.-H. Concerning effects of inert carrier gas on densities of active species and ZrO_2 etching kinetics in chlorine plasma. *ChemChemTech [Izv. Vyssh. Uchebn. Zaved. Khim. Khim. Tekhnol.]*. 2024. V. 67. N 11. P. 40–54. DOI: 10.6060/ivkkt.20246711.7073.

CONCERNING EFFECTS OF INERT CARRIER GAS ON DENSITIES OF ACTIVE SPECIES AND ZrO_2 ETCHING KINETICS IN CHLORINE PLASMA

A.M. Efremov, S.A. Smirnov, V.B. Betelin, K.-H. Kwon

Alexander M. Efremov (ORCID 0000-0002-9125-0763) *

Molecular Electronics Research Institute (MERI), Academic Valiev st., 6/1, Zelenograd, Moscow, 124460, Russia
E-mail: amefremov@mail.ru *

Sergey A. Smirnov (ORCID 0000-0002-0375-0494)

Ivanovo State University of Chemistry and Technology, Sheremetevskiy ave., 7, Ivanovo, 153000, Russia
E-mail: sas@isuct.ru

Vladimir B. Betelin (ORCID 0000-0001-6646-2660)

SRISA RAS, Nakhimovsky ave., 36, bld. 1, Moscow, 117218, Russia
E-mail: betelin@niisi.msk.ru

Kwang-Ho Kwon (ORCID 0000-0003-2580-8842)

Korea University, 208 Seochang-Dong, Chochiwon, Korea, 339-800
E-mail: kwonkh@korea.ac.kr

In this work, we investigated the influence of inert carrier gas on electro-physical plasma parameters, steady-state densities of active species and kinetics of their interaction with ZrO_2 under the condition of "soft" reactive-ion etching in chlorine. This regime assumes the lower-than-usual negative bias voltage in order to reduce both ion bombardment energy and etched surface damage. The combination of plasma diagnostics by Langmuir probes and 0-dimensional plasma modeling allowed one to analyze formation and decay kinetics for neutral and charged species at various gas mixing ratios. It was found that the mixing of Cl_2 with Ar or He at constant total gas pressure a) causes an increase in both electron temperature and plasma density; b) increases the Cl_2 dissociation degree through the acceleration of electron-impact processes; and c) intensifies the ion bombardment by the change of ion flux. From etching experiments, it was found also that the ZrO_2 etching rate is mostly composed by its chemical component, but does not correlate with the change in the Cl atom flux. The latter reveals that a) the dominant ZrO_2 etching mechanism is the ion-assisted chemical reaction and b) an increase in the effective reaction probability toward Ar or He rich plasmas reflects the acceleration of ion-induced heterogeneous effects, such as the destruction of Zr-O bonds and/or the desorption of low-volatile $ZrCl_x$ compounds. The lower neutral/charged ratio obtained in Ar-containing plasma allows one to assume the more anisotropic etching. It was shown that above findings are surely valid in the pressure range of 4–12 mTorr as well at bias powers of 100 – 300 W.

Keywords: Cl_2, Ar, plasma, parameters, active species, ionization, dissociation, etching, reaction probability

INTRODUCTION

Reactive-ion etching (RIE) processes are the well-known tools for "dry" cleaning and patterning of numerous materials used in the microelectronic device technology. The main idea of RIE is to combine physical (the sputtering of surface atoms by energetic ions) and chemical (the gasification of surface atoms in a form of volatile reaction products) etching pathway that provides the flexible adjustment of output process characteristics [1-3].

Though historically the dominant role in RIE technology belongs to fluorine-containing gases, there

are many materials which form very low or non-volatile fluorides at typical process temperatures. Nearest examples are III-V group semiconductors (GaAs, InP) and some metals (Cu, Al, Mo, Ti) used for interconnection purposes. That is why corresponding etching processes are frequently realized using chlorine-based gas chemistries, and particularly with Cl_2 plasma [4, 5]. The main feature of Cl_2 plasma under typical RIE conditions (gas pressures below 10 mtor and plasma densities above 10^{10} cm^{-3} [5]) is high dissociation degree for chlorine molecules that surely leads to [Cl] >> [Cl_2] [6]. Accordingly, an excess of etchant species causes extremely high etching rates, results in the nearly isotropic etching profile, increases surface roughness [2, 3] as well as damages reactor chamber and pumping equipment. In order to reduce above effects, Cl_2 is always combined with noble carrier gas, mostly with Ar. That is why many experimental and theoretical works were focused on various aspects of plasma chemistry and etching kinetics in Cl_2 + Ar gas mixture, including effects of gas mixing ratio [7-11]. The most important findings were that the addition of Ar a) disturbs the electron energy distribution function; b) influences the ionization/recombination balance resulting in increasing plasma density; and c) intensifies both chemical and the physical etching pathways through the growth of ion flux. All these allow one to use Ar-rich gas mixture without the loss in plasma chemical activity. On this background, the much less attention was attracted to Cl_2 + He plasma, and there are no studies where these two carrier gases were compared under identical operating conditions. At the same time, the interest to He is due to high heat conductivity coefficient [12] that provides the effective heat transfer from gas to chamber walls. Obviously, this flattens gas temperature and density profiles that may be important for increasing etching uniformity. Therefore, the comparative study of Cl_2 + Ar and Cl_2 + He plasmas is the somewhat important task to ensure the correct choice of carrier gas according to given process requirements.

Another important feature of modern times is that the electronic device technology involves many new materials with advanced characteristics. One of such materials is ZrO_2 which exhibits high (above 20) dielectric constant, a wide (above 5 eV) and close thermal expansion coefficient with silicon [13, 14]. All these mean that ZrO_2 has the evident potential to replace silicon-based dielectrics in gate structures of field-effect transistors. Previously, several authors have attempted to investigate the features of ZrO_2 etching process using various gas chemistries, including chlorine-containing gases (see, for example, Refs. [15-18]). In the last case, the principal findings were that a) the etching kinetics corresponds to ion-flux-limited regime and is characterized by typical rates of tens nm/min; b) the etching process is accelerated in the presence of BCl_3; and c) the plasma-treated surface is always contaminated by $ZrCl_x$ compounds. Unfortunately, most of existing works had the purely experimental nature and thus, did not provide the analysis of obtained effects in connection with plasma parameters and plasma chemistry. In such situation, any conclusions on etching mechanisms have the rather suggestive value and may be valid for a given reactor only. Therefore, the understanding of etching mechanisms and optimization of RIE regimes for ZrO_2 thin films remain to be an important task to improve the technology and thus, to increase the final device performance.

The general idea of given work was to compare Cl_2 + Ar and Cl_2 + He plasmas as sources of active species as well as to investigate how corresponding differences (if those really do exist) are reflected on ZrO_2 etching process under “soft” RIE conditions. The “soft” RIE assumes the lower-than-usual negative bias voltage in order to reduce both ion bombardment energy and etched surface damage. In fact, the similar task was the subject of our previous study [19] and some reasonable conclusions in respect to both plasma chemistry and etching kinetics have been made. At the same time, the weakness of above study is the low attention to details which may be important for both verification of model-predicted data and interpretation of various process mechanisms. Particularly, the somewhat critical points are a) no data and discussion on charged species kinetics and ionic composition; b) no comparison between model-predicted and measured Cl atom densities, except their relative trends; and c) no understanding of both contributions of physical and chemical etching pathway to the total ZrO_2 etching rate and behavior of effective probability of ion-assisted chemical reaction. At the same time, the latter brings the valuable information about external factors influencing etching kinetics and determining the etching mechanism. In addition, Ref. [19] reported on effects produced by only one variable parameter and for the reactor with quarts chamber wall that is not typical for modern RIE equipment. Obviously, such situation limits the applicability of corresponding data for the real etching process control. That is why the main focus of given study was to clean-up above questions in order to improve the knowledge on the selected combination of gas system and etched material. Another topic of essential interest was to compare both plasma parameters and ZrO_2 etching kinetics obtained with different chamber wall materials. Accordingly, experiments discussed below were conducted in the same with Ref.

[19] etching reactor (except the Al_2O_3 side wall instead of the quartz one) as well as covered the same range of processing conditions.

EXPERIMENTAL AND MODELING DETAILS

Experimental setup and conditions

Both plasma diagnostics and etching experiments were performed in the planar inductively-coupled plasma (ICP) reactor known from our previous works [7, 20]. Reactor had cylindrical (r = 16 cm, l = 13 cm) chamber made from anodized aluminum. The top side of the chamber was sealed by 20 mm-thick quartz window, and the flat 5-turn copper coil was located above it. The bottom side was limited by the chuck electrode used as a wafer holder. Plasma was excited in Cl_2 + Ar and Cl_2 + He gas mixtures using the 13.56 MHz power supply at constant total gas flow rate (q = 40 sccm) and input power (W = 600 W). Variable parameters were represented by gas pressure (p = 4-12 mtor) and chlorine/inert gas mixing ratio which was set by adjusting partial gas flow rates for mixture components. In the first experimental series, the gas pressure was fixed at p = 6 mtor while an increase in the carrier gas flow rate from 0-32 sccm corresponded to the transition from pure Cl_2 to 20% Cl_2 + 80% Ar or He gas mixture. In the second experimental series, we took gas mixtures with 60% of carrier gas and varied the gas pressure in the range of 4-12 mtor.

Electro-physical plasma parameters were obtained by a double rf-compensated Langmuir probe (LP) with using the DLP2000 (Plasmart Inc.) tool. The probe head was installed through the chamber wall-side view port, placed at 4 cm above the chuck electrode and centered in the radial position. The treatment of measured current-voltage (I-V) curves was based on well-known statements of Langmuir probe theory for low pressure plasmas [5, 21]. As a result, we obtained electron temperature (T_e) and ion current density (J_+). One and the same experiment was reproduced up to 5 times with the averaging of corresponding data.

Steady-state densities of Cl atoms were determined by the optical emission spectroscopy (OES) in a combination with the conventional actinometry approach [22, 23]. For this purpose, plasma emission spectra were monitored using the grating spectrometer AvaSpec-3648 (JinYoung Tech) in the range of 200-800 nm. For analytical purposes, we selected two well-known atomic lines, such as Ar 750.4 nm (ε_{th} = 13.5 eV) and Cl 754.7 nm (ε_{th} = 10.6 eV). Since the Cl_2 + Ar plasma already contains a known amount of Ar ([Ar] = $= y_{Ar}N$, where $N = p/k_BT_{gas}$ is the gas density at the temperature of T_{gas}), no special actinometer gas was needed. In the case of Cl_2 + He plasma, we additionally introduced 2 sccm of Ar that corresponded to y_{Ar} = = 4.8% Ar. In preliminary LP experiments, it was found that the given amount of Ar does not disturb plasma parameters (at least, in the extend exceeding the standard experimental error) and thus, does not influence the Cl atom kinetics. Previously, several works have mentioned that the excited state corresponded to Cl 754.7 nm line (as well as for any other line appearing in the "red" region of 700-800 nm) may also be populated by the dissociative excitation of Cl_2 molecules [24, 25]. When summarizing existing data, one can understood that a) the contribution of last process to the total Cl atom excitation rate decreases with increasing dissociation degree for Cl_2 molecules, α; and b) when neglecting the dissociative excitation, the formally acceptable error of 10% or less requires $\alpha \sim$ 30-35% or more that corresponds to [Cl] > [Cl_2]. According to Refs. [26-28], the last condition is a kind of typical case for low-pressure (p < 20 mTorr) and high-density ($n_e > 10^{10}$ cm^{-3}) Cl_2 plasmas. That is why Hsu et al. [29] reported the fairly good agreement between Cl atom densities measured by mass-spectrometry and optical actinometry using Ar 811.5 nm (ε_{th} = 13.1 eV) and Cl 725.7 nm (ε_{th} = 10.4 eV) lines at p = 10 mTorr and W = 150 W that corresponded to $n_e \sim 3\times10^{10}$ cm^{-3}. Taking into account that our processing conditions also normally provide $n_e > 10^{10}$ cm^{-3} and [Cl]/[Cl_2] > 1 [7, 20], we determined the Cl atom density as

$$[Cl] = y_{Ar}NC_a(I_{Cl}/I_{Ar}), \quad (1)$$

where I are measured emission intensities, and C_a = $= (\lambda_{Ar}k_{ex,Cl}A_F)/(\lambda_{Cl}k_{ex,Ar}A_{Ar})$ is the actinometrical coefficient that depends on corresponding wavelengths (λ), excitation rate coefficients (k_{ex}) and optical transition probabilities (A). Excitation cross-sections for Cl and Ar atoms needed to calculate k_{ex} were taken from Refs. [23, 30].

For etching experiments, we used fragments of Si(100) wafer with preliminary deposited 130-nm thick ZrO_2 film. The film was produced by the plasma-enhanced atomic layer deposition (PEALD) method described in Ref. [31]. Etched samples with an average size of ~ 2×2 cm were placed in the center of the chuck electrode. The low sample size allowed one to neglect both loading effect and disturbance of plasma parameters by the etching products. Accordingly, we obtained no differences in ZrO_2 etching rate and plasma diagnostics data with increasing number of loaded samples. The chuck electrode was equipped by the water-flow cooling system that stabilized its temperature at ~ 20 °C during the "plasma on" time. In addition, the electrode was powered by an independent rf 13.56 MHz generator to produce the negative bias voltage. The bias

power W_{dc} was varied in the range of 100-300 W in order to adjust the negative dc bias voltage and thus, to control the ion bombardment energy. The beginning of this range was especially set to be lower than typical values used for RIE processes of other materials [4, 5]. The main goal was to cover the so-called "soft" etching condition featured by reduced ion bombardment energy in order to minimize surface damage. In fact, this is a kind typical requirement which helps to avoid the degradation of dielectric properties for high-k dielectrics [13]. The ZrO_2 etching rates were determined as $R = \Delta h/\tau$, where τ is the processing time, and Δh is the etched depth. The latter was measured using a surface profiler (Alpha-step 500, Tencor). For this purpose, we developed the line striping of the photoresist AZ1512 with the line/space ratio of 2 μm/2 μm.

0-Dimensional plasma model

To obtain the information on densities of plasma active species, we applied a simplified 0-dimensional (global) model. The latter solved the system of chemical kinetic equations in the seven-component approximation (Cl_2, Cl_2^+, Cl, Cl^+, Cl^-, X and X^+, where X = Ar or He) with using the LP diagnostics data as input parameters. As outputs, the model yielded steady-state densities of plasma active species and their fluxes at the plasma/surface interface. Both modeling algorithm and kinetic scheme (the set of reactions with corresponding rate coefficients) were verified in our previous works [10, 32, 33]. Basic assumptions were as follows:

1) The electron energy distribution function (EEDF) has the nearly Maxwellian shape. The reason is the sufficient role of equilibrium electron-electron collisions under the condition of high ionization degree for gas species ($n_+/N > 10^{-4}$, where n_+ is the total positive ion density). Accordingly, rate coefficients for electron-impact reactions appear in a simple algebraic form of $k = AT_e^B\exp(-C/T_e)$ after the integration of Maxwellian EEDF with known process cross-sections [7, 34].

2) The relationship between measured J_+ and total density of positive ions is assumed as $J_+ \approx \approx 0.61en_+(eT_e/m_i)^{1/2}$ [5], where m_i is the effective ion mass. The last parameter may be evaluated through individual masses of dominant positive ions, as was suggested in Refs. [10, 32].

3) The heterogeneous loss of Cl atoms follows the first-order kinetics with the nearly constant recombination probability, γ_R. The indirect proof is the nearly constant temperature of external chamber wall that allows one to expect the negligible change in the internal wall temperature. At the same time, we accounted for the weak sensitivity of γ_R to $[Cl]/[Cl_2]$ ratio, as was suggested in Refs. [28, 35].

Approaches for the analysis of etching kinetics

Basic features of heterogeneous processes kinetics under reactive-ion etching conditions in non-polymerizing halogen-containing plasmas have been discussed in several works [19, 36-38]. Corresponding conclusions in the framework of our case may briefly be summarized as follows:

1) Measured etching rate R represents the superposition of physical sputtering (R_{phys}) and heterogeneous chemical reaction with chlorine atoms (R_{chem}). The second component may appear in either spontaneous or ion-assisted forms depending on the nature of both etched material and reaction products.

2) The rate of physical sputtering (as well as the rate of ion-stimulated desorption of low volatile reaction products) $R_{phys} = Y_S\Gamma_+$, where Y_S is the process yield (particle per incident ion), and $\Gamma_+ \approx \approx h_Ln_+(eT_e/m_i)^{1/2}$ is the ion flux. The dimension-less correction factor for the ion density on the plasma sheath edge h_L is given by the low-pressure diffusion theory [5]. Taking into account that Y_S is proportional to momentum transferred from incident ion to the surface atom [39], the relative change in R_{phys} may be traced by the parameter $(m_i\varepsilon_i)^{1/2}\Gamma_+$ characterizing the ion bombardment intensity. The required ion bombardment energy ε_i may be evaluated as $\varepsilon_i = e|-U_{dc}-U_p|$, where $-U_{dc}$ is the negative dc bias voltage, and $-U_p$ is the plasma potential [5].

3) The rate of heterogeneous chemical reaction $R_{chem} = \gamma_R\Gamma_{Cl}$, where $\Gamma_{Cl} \approx 0.25[Cl](RT_{gas}/\pi M_{Cl})^{1/2}$ is the Cl atom flux, and γ_R is the effective reaction probability. The latter mainly depends on the surface temperature, but may also be sensitive to the ion bombardment intensity. Corresponding mechanisms which produce somewhat opposite effects are a) the ion-stimulated desorption of etchant species in prior to their interaction with surface atoms; and b) the production of free adsorption sites for etchant species due to both breaking chemical bonds between surface atoms and sputtering of low volatile reaction products.

RESULTS AND DISCUSSION

Fig. 1 illustrates how variable processing conditions influence electrons- and ions-related plasma parameters. In preliminary experiments, it was found that the change in bias power from 100-300 W at W, p = const does not disturb both raw I-V curves and derived data. In fact, this phenomenon reflects the basic feature of ICP etching system to provide the independent control for ion flux and ion energy [5]. That is why only the data related to the content of carrier gas and gas pressure are plotted. Though the effect of pressure

itself is not a principal focus of this study, corresponding data may be useful to demonstrate that findings related to carrier gases are valid not only for a single combination of processing conditions. In addition, as most of effects exhibit similar trends with those obtained earlier for Cl_2 + Ar plasmas [6-10], below we provide only brief comments with attracting the attention to differences between two gas systems:

1) Electron temperature exhibits the growth with increasing content of carrier gas (Fig. 1(a)), but decreases toward higher gas pressures (Fig. 1(c)). The general reason for the first effect is a decrease in the overall electron energy loss due to decreasing fraction of molecular component. Really, Cl_2 molecules are featured by the very wide electron energy loss window starting from their dissociation threshold of ~ 3.0 eV [40, 41]. At the same time, first excitation potentials for both Ar (~ 11.8 eV) and He (~ 19.8 eV) atoms appear to be much higher while corresponding process are characterized by lower cross-sections [41]. That is why the dilution of chlorine by any carrier gas shrinks the electron energy loss range, lowers the energy exchange in a single collision and finally results in increasing fraction of high-energy electrons in EEDF. Accordingly, the stronger growth of T_e in He-containing plasma is due to lower energy losses for both excitation and ionization of He compared with those for Ar. The change of T_e vs. gas pressure surely reflects an increase in electron energy losses due to increasing both gas density and electron-neutral collision frequency. In fact, this is a kind of universal rule of plasma chemistry that does work independently on the type of working gas [5].

2) Density of electrons demonstrates an increase toward Ar- and He-rich plasmas (Fig. 1(b)), but decreases vs. gas pressure (Fig. 1(d)). The phenomenon of Ar and He contents becomes to be clear when accounting for corresponding process kinetics represented in Fig. 1(e). In Cl_2 + Ar plasma, the total ionization frequency $\nu_{iz} = k_1[Cl_2] + k_2[Cl] + k_3[Ar]$, where k are rate coefficients for R1: $Cl_2 + e \rightarrow Cl_2^+ + 2e$, R2: $Cl + e \rightarrow Cl^+ + 2e$ and R3: $Ar + e \rightarrow Ar^+ + 2e$, keeps the nearly constant value at 0–80% Ar. The reason is that a bit lower rate coefficient for R3 (~ 2.4×10^{-10} cm^3/s compared with ~ 1.3×10^{-9} cm^3/s for k_1 and ~ 6.8×10^{-10} cm^3/s for k_2) is compensated by its stronger growth vs. T_e due to higher threshold energy. Simultaneously, the rather small change in diffusion loss frequency ν_{dif} meets the drastic fall in attachment frequency $\nu_{da} = k_4[Cl_2]$ (where R4: $Cl_2 + e \rightarrow Cl + Cl^-$) due to decreasing content of Cl_2 in a feed gas and increasing its dissociation degree. Taking into account that $\nu_{da} \approx \nu_{dif}$ in pure Cl_2 plasma, such situation corresponds to a sufficient decrease in the total electron loss frequency and thus, causes the nearly proportional increase in n_e (by ~ 14 times for 0-80% Ar). In the Cl_2 + + He plasma, where the stronger increase in T_e takes place, the parameter ν_{iz} also demonstrates the noticeable growth, mostly due to changes in k_1 (2.4×10^{-10}-4.3×10^{-9} cm^3/s at 0-80% He) and k_2 (1.1×10^{-10}-3.2×10^{-9} cm^3/s at 0-80% He). The contribution of third summand, k_5[He], where R5: $He + e \rightarrow He^+ + 2e$, appears to be much lower due to $k_5 << k_1, k_2$. At the same time, ν_{dif} also exhibits the strong growth following an increase in the electron diffusion coefficient $D_e = f(T_e)$. Such situation rapidly yields $\nu_{dif} >> \nu_{da}$, so that a decrease in ν_{da} has the only weak effect on the total electron loss frequency. That is why n_e exhibits the much weaker sensitivity to the content of carrier gas demonstrating an increase by only ~ 4 times for 0-80% He. As for the effect of gas pressure, it has the similar mechanism for both gas systems. In particular, the transition toward higher pressures always lowers ν_{iz} (3.7×10^4-1.9×10^4 s^{-1} at 0-80% Ar and 3.7×10^4-2.4×10^4 s^{-1} at 0-80% He, due to a decrease in all ionization rate coefficients together with T_e) as well as causes an increase in ν_{da}, as an increase in the density of source species for R4 takes place. Accordingly, this corresponds to both decrease in electron formation and increase in electron loss rate.

3) The total density of positive ions (Fig. 1(b, d)) always follows the behavior of n_e, but also reflects the change in plasma electronegativity. In particular, decreasing gap between n_+ and n_e toward Ar and He-rich mixtures (Fig. 1(b)) is due to decreasing n_-/n_e (2.4-0.01 at 0-80% Ar and 2.4-0.07 at 0-80% He) that finally leads to $n_+ = n_e$ in pure noble gas plasmas. Accordingly, the slower change in n_+ compared with n_e vs. gas pressure results from a decrease in both relative (0.06-0.38 in Cl_2 + Ar plasma and 0.14-1.19 in Cl_2 + He plasma at 4-12 mtor) and absolute (1.0×10^{10}-4.4×10^{10} cm^{-3} in Cl_2 + + Ar plasma and 1.4×10^{10}-5.3×10^{10} cm^{-3} in Cl_2 + He plasma at 4-12 mtor) density of Cl^- ions. In both cases, the reason is corresponding change in the rate of R4 matched with the density of Cl_2 molecules. The total flux of positive ions always follows the behavior of n_+, but exhibits a bit stronger absolute change vs. both gas mixing ratios and pressure. The reason is the synergetic effect from ion Bohm velocity, $(eT_e/m_i)^{1/2}$. From Fig. 1(f), it can be seen also that the density of He^+ ions is much smaller compared with that for Ar^+ under one and the same plasma excitation conditions. The reason is that $k_5 << k_3$ due to sufficient difference in ionization thresholds (15.8 eV for Ar vs. 24.6 eV for He [40, 41]). Therefore, it can be understood that effective ion masses in both gas systems are quite close.

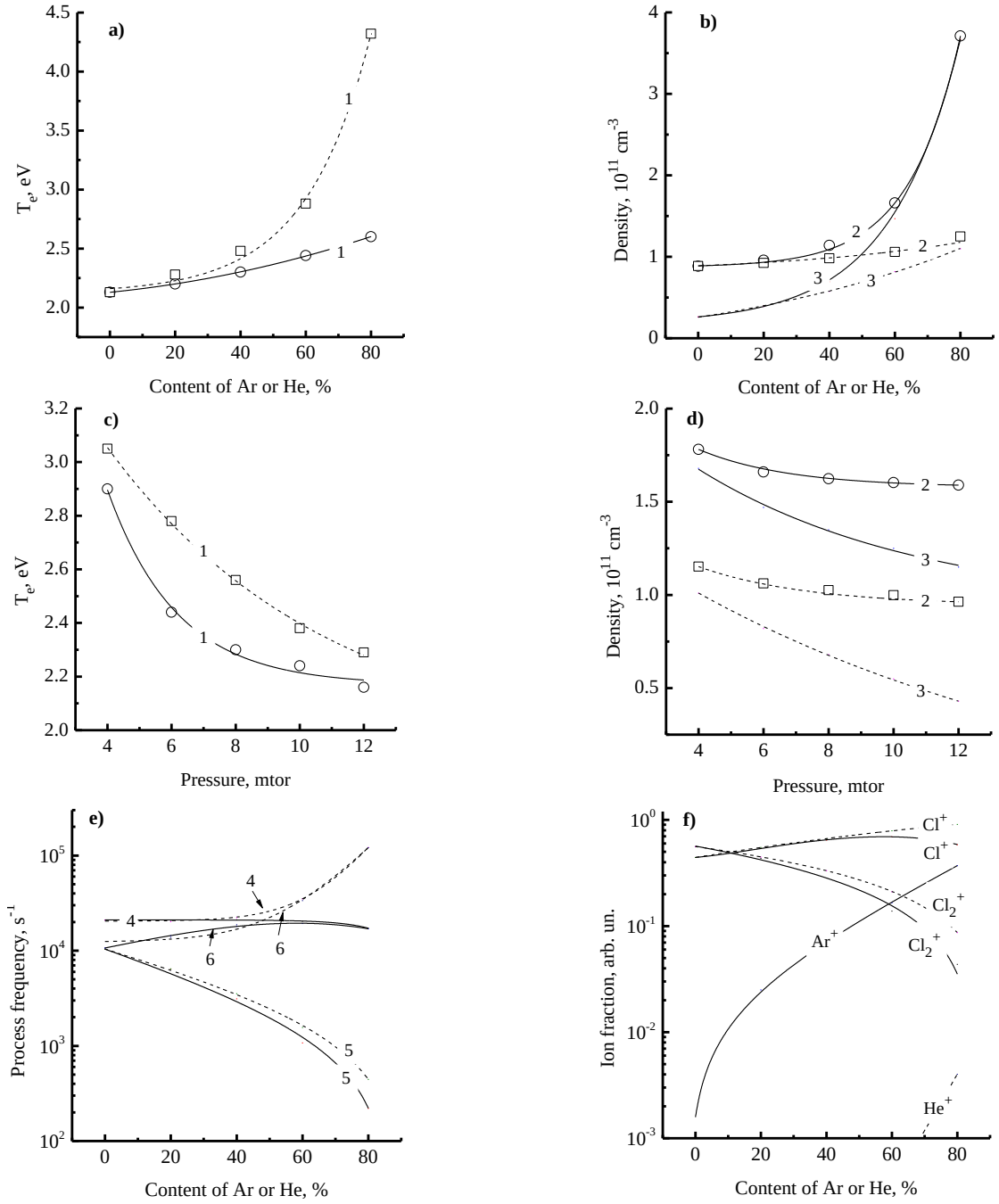

Fig. 1. Electrons- and ions-related plasma parameters in Cl_2 + Ar (solid lines) and Cl_2 + He (dashed lines) mixtures as functions of carrier gas fraction (a, b, e, f) and gas pressure (c, d): a, c) electron temperature (1); b, d) densities of charged species (2 – total positive ion density; 3 – electron density); e) process frequencies characterizing the charged species balance (4 – total ionization frequency; 5 – electron attachment frequency; 6 – diffusion loss frequency); and f) partial densities of ions inside n_+

Рис. 1. Параметры электронной и ионной компонент плазмы в смесях Cl_2 + Ar (сплошные линии) и Cl_2 + He (пунктирные линии) в зависимости от доли газа-носителя (a, b, e, f) и давления (c, d): a, c) температура электронов (1); b, d) концентрации заряженных частиц (2 – суммарная концентрация положительных ионов; 3 – концентрация электронов); e) частоты процессов формирующих баланс заряженных частиц (4 – суммарная частота ионизации; 5 – частота диссоциативного прилипания; 6 – частота диффузионной гибели); и f) парциальные концентрации ионов внутри n_+

The comparison of plasma diagnostics data from Fig. 1(a, b) with those reported in Ref. [19] indicate that all these are very close. Obviously, such situation means no differences in both electron energy loss channels and charged species kinetics that may take place only if the wall material does not influence steady-state densities of Cl_2 and Cl species. Formally, this conclusion contradicts with Kota et al. [42] where the more than five-time difference between Cl atom recombination probabilities on quarts (~ 0.03) and Al_2O_3

(~ 0.2) surfaces was obtained. At the same time, one must remember that Kota's measurements were conducted under non-plasma conditions in experiments with Cl atom beams. The latter means that the surface was attacked by only one type of species as well as was not conditioned by plasma-related factors, such as ion bombardment, UV irradiation, etc. In spite of this, several articles demonstrated that Cl atoms recombination probabilities on both stainless steel [35, 43] and Al_2O_3 [43] under the Cl_2 plasma condition are much lower than those reported in Ref. [42] and appear to be sensitive to $[Cl]/[Cl_2]$ ratio. The reason is the competitive adsorption of Cl_2 molecules that reduces the fraction of free adsorption sites for atomic species. In particular, Ref. [43] reported the Cl atom recombination probability of ~ 0.03 for Al_2O_3 at $[Cl]/[Cl_2] \sim 0.5$ as well as allows the prediction of 0.05–0.07 for $[Cl]/[Cl_2] > 1$. As a confirmation, namely these values provide the satisfactory agreement between our model-predicted Cl atoms densities with those obtained after the actinometry procedure. From Ref. [43], it can be understood also that the above effect does not work for quartz surface, probably due to the very low adsorption probability for Cl_2 molecules. Oppositely, the exposure in plasma increases the Cl atom recombination probability up to 0.04-0.05 due to both increasing surface roughness and formation of $SiCl_xO_y$ layer on plasma/surface interface. Therefore, as plasma "equalizes" Cl atom recombination probabilities on quartz and Al_2O_3 surfaces, the steady-state densities of Cl_2 and Cl species in two reactors featured by only different side wall materials also appear to be very close. As such, the similarity of Langmuir probe data mentioned above has received the reasonable explanation.

As the ZrO_2 etching process is driven by the ion bombardment [15–18], the question of primary importance is how processing conditions do influence the ion bombardment intensity. From Fig. 2(a), it can be seen that the negative dc bias voltage is almost identical (within the standard experimental error, of cause) for both Ar- and He-containing plasmas. In fact, this confirms the model-based conclusion concerning close effective ion masses. The non-constant $-U_{dc}$ is because the negative charge induced at W_{dc} = const is partially compensated by positive ion coming from bulk plasma. That is why the absolute value of $-U_{dc}$ always changes oppositely to Γ_+, i. e. decreases with increasing fraction of carrier gas and increases vs. gas pressure. Another remarkable fact is that the relative change in Γ_+ appears to be stronger compared with $-U_{dc}$. Therefore, the parameter $\varepsilon_i^{1/2}\Gamma_+$ which traces the ion bombardment intensity under the condition of $m_i \approx$ $\approx$ const [44] follow the behavior of Γ_+, as shown in Fig. 2(b). An increase in bias power causes the nearly linear growth of negative bias voltage which appears to be a bit stronger in Cl_2 + Ar plasma (Fig. 2(c)). This effect is enforced by the similar difference in ion fluxes, so that the parameter $\varepsilon_i^{1/2}\Gamma_+$ exhibits noticeably higher absolute values with Ar as a carrier gas (Fig. 2(d)). The relatively low sensitivity of $\varepsilon_i^{1/2}\Gamma_+$ to bias power is because only the factor of $\varepsilon_i^{1/2}$ does work at Γ_+ = const. When summarizing above data, one can conclude that the Cl_2 + Ar plasma with more than 50% carrier gas provides better conditions for ion-induced heterogeneous process compared with the He-containing counterpart. The similar conclusion indirectly follows from data of Ref. [19].

An important summary delivered by Fig. 1 is that a) the dilution of chlorine by Ar or He causes qualitatively similar changes in plasma parameters determining the dissociation kinetics of Cl_2 molecules; and b) the quantitative differences between Ar- and He-containing plasmas keep their typical features in all investigated range of gas pressures. Therefore, one can surely suggest no principal differences in behaviors of Cl atom densities. When analyzing kinetics of neutral species, we confirmed all principal features of Cl_2 plasma reported in previous works. In particular, it was found that the dominant Cl atom formation pathway is R6: $Cl_2 + e \rightarrow 2Cl + e$ while contributions of dissociative attachment R4 and dissociative ionization R7: $Cl_2 + e \rightarrow Cl + Cl^+ + 2e$ are much lower. The reason is the difference in corresponding rate coefficients ($\sim 1.1\times10^{-8}$ cm^3/s for k_6 vs. $\sim 2.4\times10^{-10}$ cm^3/s for k_4 and $\sim 2.2\times10^{-11}$ cm^3/s for k_7 at T_e = 3 eV) resulting in $2k_6 >> k_4 + k_7$. Therefore, the effective dissociation rate coefficient for Cl_2 molecules is $k_{dis} \approx k_6$. It was found that the parameter k_{dis} increases toward Ar- and He-rich plasmas (by ~ 1.3 and 2.4 times, respectively, at 0-80% carrier gas) as well as decreases with increasing gas pressure. Both effects are in agreement with trends and absolute difference in electron temperatures, as was mentioned in Figs. 1(a, c). As the dilution of chlorine by both Ar and He also causes a growth of electron density, one can obtain a sufficient increase in the frequency of dissociative collisions for electrons with Cl_2 molecules (Fig. 3(a)) and Cl_2 dissociation degree (Fig. 3(b)). The result is the slower-than-linear decrease in Cl atom density (by ~ 1.3 times at 0-50% Ar and by ~ 1.4 times at 0-50% He, as follows from plasma modeling results shown in Figs. 3(d, f)). Similar situation has repeatedly been mentioned in published works for Cl_2 + Ar plasmas excited using both direct-current and radio-frequency power sources [6, 32, 33]. Oppositely, an increase in gas pressure lowers the electron density and thus, enforces the retarding effect

of k_{dis} in respect to the Cl_2 dissociation rate. As a result, a decrease in Cl_2 dissociation degree (Fig. 3(b)) produces the slower-than-proportional increase in Cl atom density. Another remarkable phenomenon is that both $k_{dis}n_e$ and $\alpha(Cl_2)$ appear to be higher in Cl_2 + Ar plasma, in spite of lower k_{dis}. The reason is the opposite and more sufficient difference in electron densities, as shown in Fig. 1(b, d). Finally, we would like to mention the acceptable agreement between measured and model-predicted Cl atom densities plotted in Fig. 3(d, f). In fact, this means that our model-based analysis provides the correct understanding of main kinetic effects determining plasma parameters and composition.

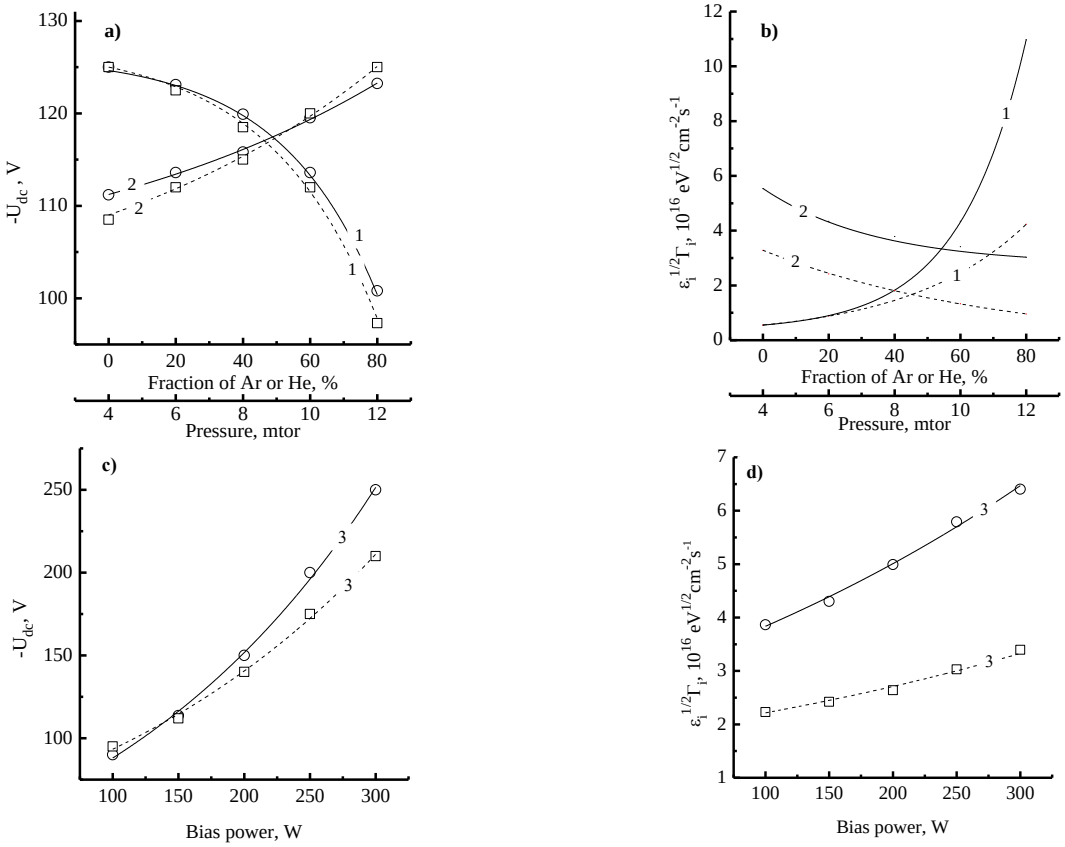

Fig. 2. Negative dc bias voltage (a, c) and parameter $\varepsilon_i^{1/2}\Gamma_+$ characterizing the ion bombardment intensity (b, d) as functions of carrier gas fraction (1), gas pressure (2) and bias power (3) in Cl_2 + Ar (solid lines) and Cl_2 + He (dashed lines) plasmas

Рис. 2. Отрицательное смещение (a, c) и параметр $\varepsilon_i^{1/2}\Gamma_+$ характеризующий интенсивность ионной бомбардировки (b, d) в зависимости от содержания газа-носителя (1), давления (2) и мощности смещения (3) в плазме Cl_2 + Ar (сплошные линии) и Cl_2 + He (пунктирные линии)

In etching experiments, it was found that the mixing of Cl_2 with Ar or He causes monotonically increasing as well as almost identical absolute values for ZrO_2 etching rates, R, up to 35-40% of carrier gas (Fig. 4(a, c)). The furthermore transition to Cl_2-poor mixtures does not change the nearly linear tendency for Cl_2 + Ar plasma while causes a kind of saturation of ZrO_2 etching rate in Cl_2 + He plasma. As a result, the latter exhibits by ~ 1.5 times slower etching at the last point corresponding to 80% He. The variation of pressure results in quite close etching rates at both low and high pressure ends, but causes a weak maximum located at p ~ 6-8 mtor. An increase in bias power (Fig. 4(e)) causes the almost proportional growth of ZrO_2 etching rate as well as leads to the slightly increasing gap between Cl_2 + Ar abd Cl_2 + He plasmas toward higher input powers. The last effect reasonable reflects the difference in ion bombardment intensities mentioned in Fig. 2(d). When comparing above data with Fig. 1(b) and 2(b), it can be understood that a) the behavior of ZrO_2 etching rate vs. fraction of carrier gas is always opposite to that for Cl atom flux while demonstrates the agreement with ion flux and ion bombardment intensity; and b) the non-monotonic change of ZrO_2 etching rate vs. gas pressure demonstrates the formal agreement with Γ_{Cl} at lower pressures as well as follows the change of Γ_+ at higher pressures. In order to understand mechanisms of above phenomena we conducted both plasma diagnostics and etching experiments in pure Ar

and He plasmas and then, evaluated ZrO_2 sputter yields, Y_{sp}, as the etching rate to ion flux ratios. Corresponding values were found to be ~ 0.001 atom/ion and ~ 0.0007 atom/ion, respectively. In our opinion, such low sputter yields are due to both low ion bombardment energies and strong Zr-O bonding (~ 766 kJ/mol [12]), so that the sputtering process occurs in the near-threshold region. Accordingly, the calculation of physical etching rate in Cl_2-containing plasma $R_{phys} = Y_{sp}\Gamma_+$ ($\Gamma_+ = 4.9\times10^{-14}$-$1.1\times10^{16}$ $cm^{-2}s^{-1}$ for 0-80% Ar and 4.9×10^{-14}-4.2×10^{15} $cm^{-2}s^{-1}$ for 0-80% He) clearly demonstrated that $R_{phys} << R$ and $R \approx R_{chem}$ (Fig. 4(a, c, e)).

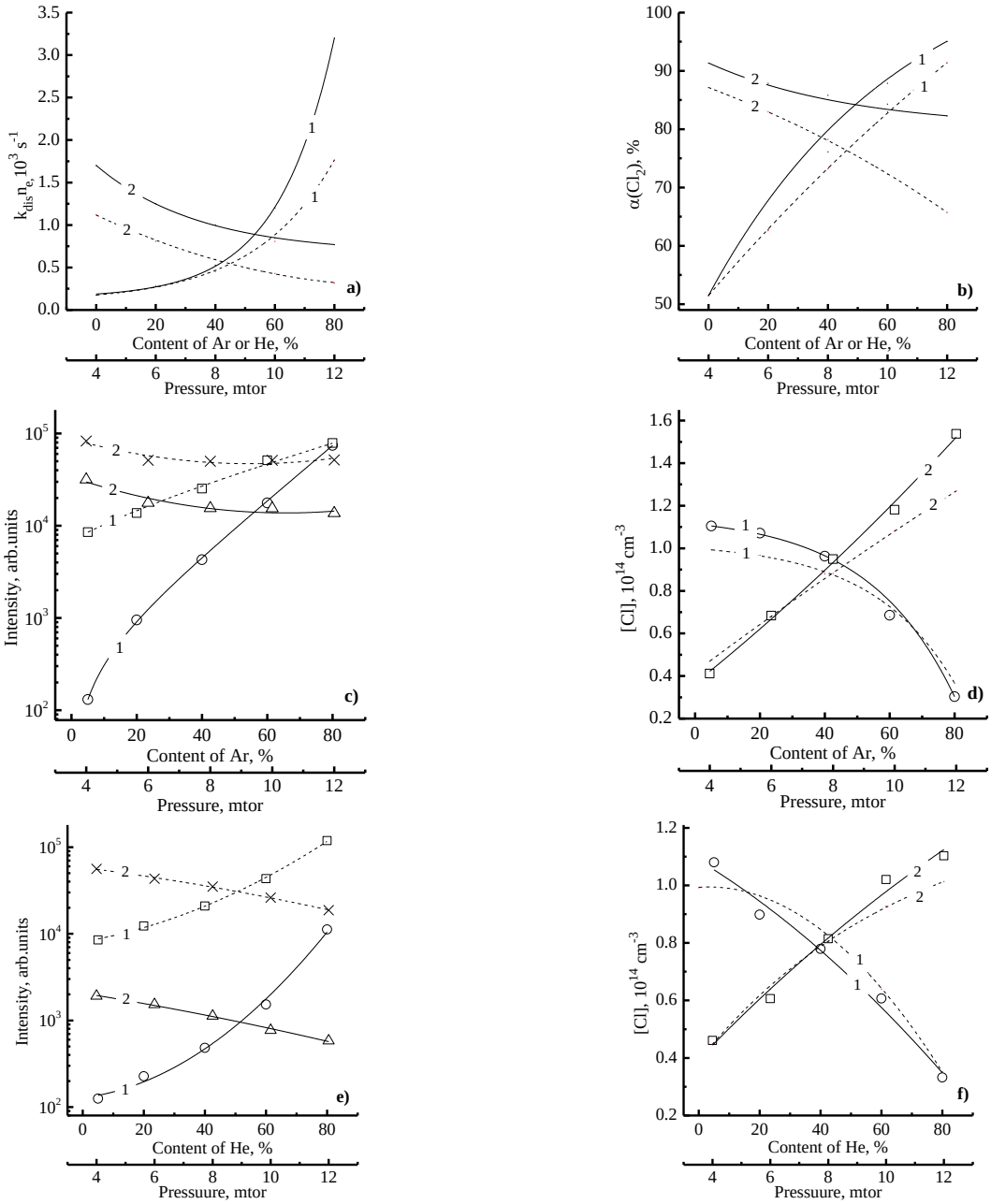

Fig. 3. Kinetics and densities of neutral species in Cl_2 + Ar and Cl_2 + He plasmas as functions of carrier gas fraction (1) and pressure (2): a) effective frequency of dissociative collisions of electrons with Cl_2 molecules; b) Cl_2 dissociation degree; c, e) emission intensities for Ar 750.4 nm and Cl 754.7 nm; d, f) measured and model-predicted densities of Cl atoms. In Figs. a) and b), solid lines for Cl_2 + Ar while dashed lines are for Cl_2 + He. In Fig. c) and e), solid lines are for Ar 750.4 nm while dashed lines are for Cl 754.7 nm. In Fig. d) and f), solid lines with symbols are from actinometry experiments while dashed lines are from plasma modeling

Рис. 3. Кинетика и концентрации нейтральных частиц в плазме Cl_2 + Ar и Cl_2 + He в зависимости от доли газа-носителя (1) и давления (2): a) эффективная частота диссоциирующих столкновений электронов с молекулами Cl_2; b) степень диссоциации Cl_2; c, e) интенсивности излучения линий Ar 750.4 nm and Cl 754.7 nm; d, f) измеренные и расчетные концентрации атомов Cl. На рис. a) и b), сплошные линии для Cl_2 + Ar, пунктирные – для Cl_2 + He. На рис. c) и e), сплошные линии для Ar 750.4 нм, пунктирные – для Cl 754.7 нм. На рис. d) и f), сплошные линии с символами представляют актинометрический эксперимент, пунктирные – расчет

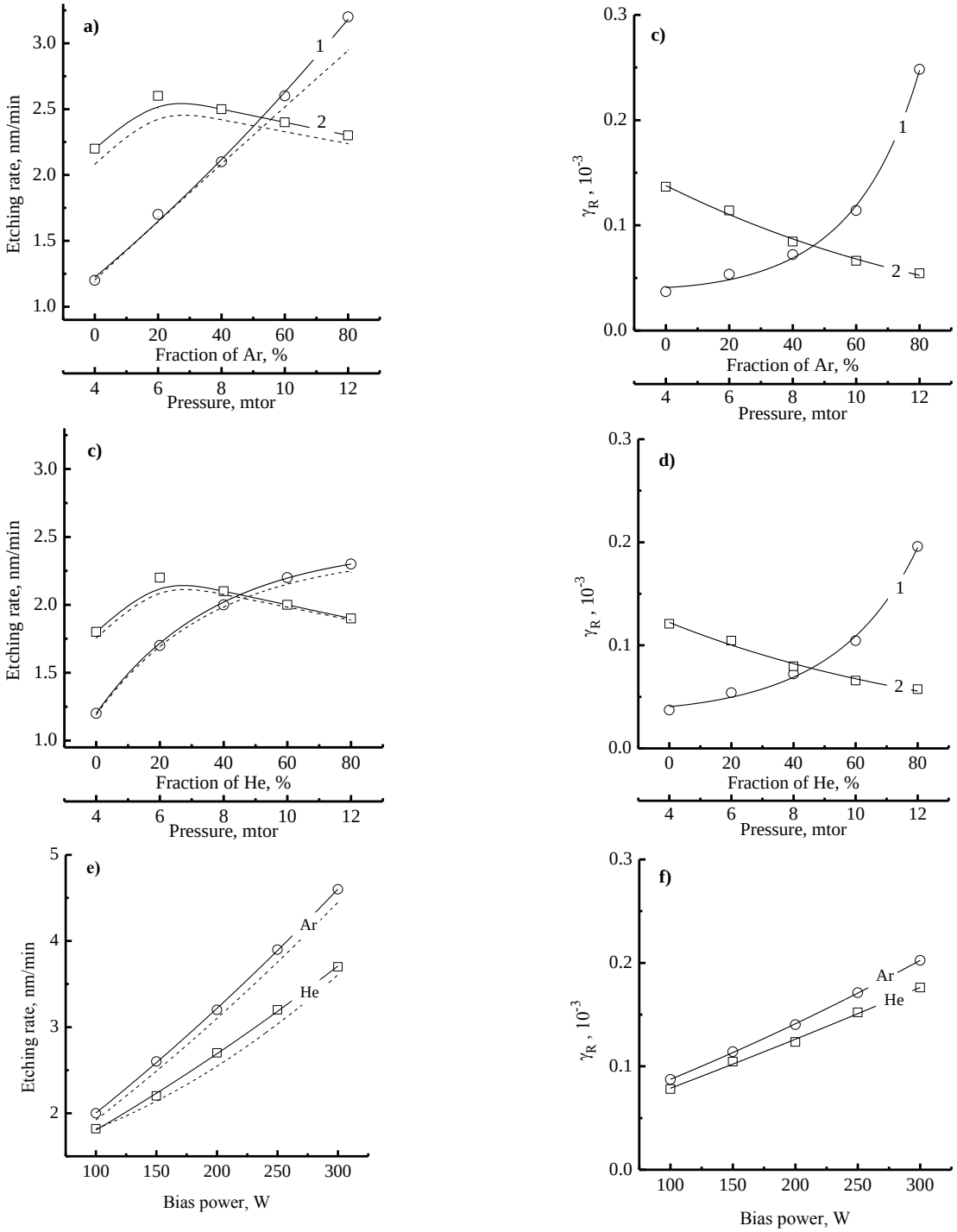

Fig. 4. ZrO_2 etching kinetics in Cl_2 + Ar and Cl_2 + He plasmas as functions of carrier gas fraction (curves 1 in a)-d)), gas pressure (curves 2 in a)-d)) and bias power (e, f). In Fig. a), c) and e) - ZrO_2 etching rate found in experiments. In Fig. b), d) and f) - effective probability of heterogeneous chemical reaction. Dashed lines in Fig. a), c) and e) represent the chemical etching component, R_{chem}
Рис. 4. Кинетика травления ZrO_2 в плазме Cl_2 + Ar и Cl_2 + He в зависимости от содержания газа-носителя (кривые 1 на рис. a)-d)), давления (кривые 2 на рис. a)-d)) и мощности смещения (e, f). На рис. a), c) и e) - измеренная скорость травления. На рис. b), d) и f) - эффективная вероятность гетерогенной химической реакции. Пунктирные линии на рис. a), c) и e) представляют химическую составляющую скорости, R_{chem}

As behaviors of ZrO_2 etching rates in both gas mixtures are completely related to the chemical etching pathway, the reason may be only that the Cl atom flux is not the single factor influencing the heterogeneous reaction kinetics. Really, the effective reaction probability $\gamma_R = R_{chem}/\Gamma_{Cl}$ demonstrates the rapid growth toward Ar- and He-rich plasma and higher bias powers as well as decreases with increasing gas pressure

(Fig. 4(c, d, f)). When comparing these data with those shown in Fig. 2(b) as well as taking in mind the constant Cl atom flux during the variation of W_{dc}, it can be understood that a) the behavior of γ_R in both gas mixtures follows the change in the ion bombardment intensity; and b) the lower ZrO_2 etching rate in Cl_2 + He plasma at more than 40% He surely reflects corresponding differences in γ_R and $\varepsilon_i^{1/2}\Gamma_+$. Moreover, one can obtain the nearly linear correlation between γ_R and $\varepsilon_i^{1/2}\Gamma_+$ while the slopes of corresponding fitting lines in Fig. 5(a, b) are quite close. Obviously, the latter means no principal differences in ZrO_2 etching mechanisms in Cl_2 + Ar and Cl_2 + He plasmas.

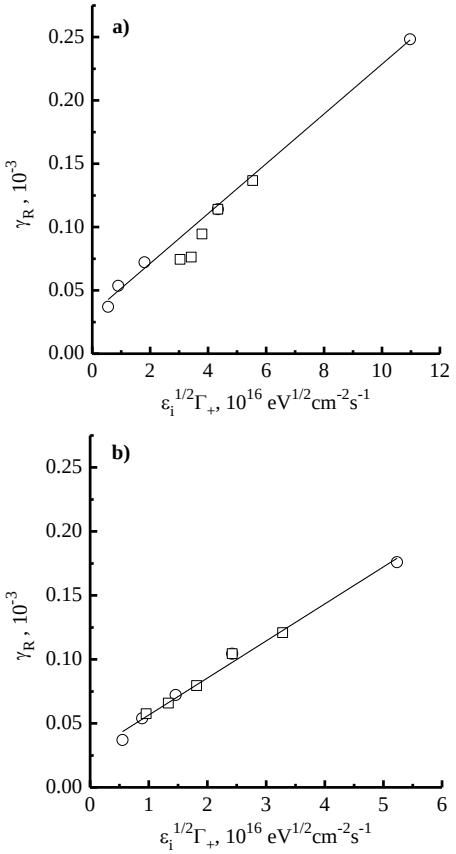

Fig. 5. The correlation between effective reaction probability and parameter $\varepsilon_i^{1/2}\Gamma_+$ characterizing the ion bombardment intensity in Cl_2 + Ar (a) and Cl_2 + He (2) plasmas

Рис. 5. Корреляция между эффективной вероятностью гетерогенной химической реакции и параметром $\varepsilon_i^{1/2}\Gamma_+$, характеризующим интесивность ионной бомбардировки, в плазме in Cl_2 + Ar (a) и Cl_2 + He (2)

In our opinion, the influence of ion bombardment on the probability of chemical reaction between Cl atoms and ZrO_2 surface appears through, at least, two mechanisms. First, the strength of Zr-O bong is sufficiently higher than for Zr-Cl one (~ 530 kJ/mol [12]), so that the spontaneous (thermally activated) chlorination in a form of R8: ZrO_x(s.) + xCl $\rightarrow$ $\rightarrow$ $ZrCl_x$(s.) + xO (where the index "(s.)" points out on the surface-bonded state of corresponding particle) requires high energy threshold and seems to be impossible at typical process temperatures. Obviously, such situation assumes the mandatory ion-assisted destruction of oxide bonds R9: ZrO_x(s.) $\rightarrow$ ZrO_{x-1}(s.) + O in prior to the reaction with chlorine atoms R10: Zr(s.) + + xCl $\rightarrow$ $ZrCl_x$(s.). And secondly, products of R10 seem to be really low volatile compounds, as their melting points sufficiently exceed typical process temperatures (~ 772 °C for $ZrCl_2$, ~ 627 °C for $ZrCl_3$ and ~ 437 °C for $ZrCl_4$ [12]). Therefore, the one more mandatory ion-induced step is the sputtering of reaction products R11: $ZrCl_x$(s.) $\rightarrow$ $ZrCl_x$ to clean the surface and to provide the access of etchant species to surface atoms. On this background, the increasing tendency of γ_R vs. both fraction of carrier gas and bias power (Fig. 4(c, d, f)) is exactly due to increasing probabilities for R9 and R11 together with the ion bombardment intensity. As this effect overcompensates a decrease in Γ_{Cl} with increasing content of Ar or He in a feed gas, the growth of ZrO_2 etching rate takes place. Oppositely, an increase in gas pressure lowers the ion bombardment intensity, suppresses both R9 and R11 as well as reduces γ_R. Accordingly, the concurrence between increasing Cl atom flux and decreasing their reaction probability produces a maximum on R = f(p) curves. Finally, we would like to note that we obtained at least 5 times lower absolute ZrO_2 etching rates compared with those reported in Refs. [17, 18] for Cl_2 + Ar plasmas under close range of processing conditions. Obviously, this effect cannot be completely related to the soft etching regime with reduced ion bombardment energy, as both reference works dealt with comparable (or, at least, a bit lower) values of negative dc bias voltage. In our opinion, the reasons are as follows. First, the higher ZrO_2 etching rates were obtained with either the electron-cyclotron resonance (ECR) plasma source [19] or conventional ICP with higher input power density [18]. In both cases, one can easily expect the higher plasma density and ion flux that results in higher efficiency of both R9 and R11. And secondly, kinetic coefficients for R9 and R10 are strongly dependent on film properties, such as surface roughness, crystal structure, stoichiometry, presence of impurities, etc. Since all these reflect features of ZrO_2 deposition method, too many factors cannot be compared adequately. Probably, the lower etching rate in our case means the low density of surface defects as well as the higher film purity and crystallinity. However, the latter is just a suggestion, not a fact.

When summarizing above data, one can conclude that there are no principal differences between Ar and He carrier gases in respect to both plasma composition and ZrO_2 etching performance. Moreover, when the fraction of carrier gas does not exceed 40%, the almost identical plasma and etching process parameters take place. Therefore, the choice between Ar and He for purposes of given etching process may be motivated by pure technological criteria, such as etching uniformity, selectivity and anisotropy issues. In the last case, the Cl_2 + Ar plasma has some formal advantage, as it is characterized by the lower impact of "chaotic" etching component due to lower Γ_{Cl}/Γ_+ ratio (3000-50 at 0-80% Ar vs. 3000-120 at 0-80% Ar). As the same time, such difference is noticeable only in noble-gas-rich plasmas as well as appears to be rather weak in Cl_2-rich plasmas.

CONCLUSIONS

In this work, we investigated how the type and the content of inert carrier gas, Ar or He, do influence plasma chemistry and ZrO_2 etching kinetics in chlorine-based plasmas. Experimental conditions corresponded to the so-called "soft" reactive-ion etching regime featured by lower-than-usual negative bias voltage and ion bombardment energy. From plasma diagnostics by Langmuir probes, it was found that increasing fraction of any carrier gas a) causes similar trends in electrons- and ions-related plasma parameters (as it follows from changes in electron energy loss channels and ionization/recombination balance for ionic species); and b) enlarges the difference between absolute values of electron temperature and plasma density. As a result, the Cl_2 + Ar plasma always exhibits higher (by ~ 2 times at 80% Ar or He) ion flux and ion bombardment intensity. An important common effect is also that the addition of Ar or He accelerates the decomposition of Cl_2 molecules in electron-impact processes, increases their dissociation degree and finally results in the slower-than-proportional decrease in the Cl atom density (by less than 3 times at 0-80% Ar or He). Etching experiments with ZrO_2 thin films indicated both domination of chemical etching pathway and sufficient growth of effective reaction probability toward Ar- or He-rich plasmas. As the latter completely correlates with increasing ion bombardment intensity, one can surely assume the ion-assisted etching regime. Accordingly, the role of ion bombardment includes a) the destruction of Zr-O bonds to provide the chlorination of Zr atoms; and b) the desorption of low volatile $ZrCl_x$ compounds. The lower neutral/charged ratio obtained in Cl_2 + Ar plasma allows one to suggest the advantage in both etching anisotropy and profile shape under the condition of Ar-rich plasma.

The publication was made within the framework of the state task of the Federal State Institution Scientific Research Institute for System Analysis, Russian Academy of Sciences (conducting fundamental scientific research (47 GP)) on the topic No. 1023032900380-3-1.2.1 "Fundamental and applied research in the field of lithographic limits of semiconductor technologies and physicochemical processes of etching 3D nanometer dielectric structures for the development of critical technologies for the production of electronic components. Research and construction of models and designs of microelectronic elements in an extended temperature range (from -6 °C to +30 °C) (FNEF-2024-0004)".

The authors declare the absence a conflict of interest warranting disclosure in this article.

Публикация выполнена в рамках государственного задания Федерального государственного учреждения «Научно-исследовательский институт системного анализа Российской академии наук» (выполнение фундаментальных научных исследований (47 ГП)) по теме № 1023032900380-3-1.2.1 «Фундаментальные и прикладные исследования в области литографических пределов полупроводниковых технологий и физико-химических процессов травления 3D нанометровых диэлектрических структур для разработки критических технологий производства электронных компонентов. Исследование и создание моделей и конструкций элементов микроэлектроники в расширенном диапазоне температур (от -6 °C до +30 °C) (ФНЕФ-2024-0004)».

Авторы заявляют об отсутствии конфликта интересов, требующего раскрытия в данной статье.

ЛИТЕРАТУРА
REFERENCES

1. **Nojiri K.** Dry etching technology for semiconductors. Tokyo: Springer Internat. Publ. 2015. 116 p. DOI: 10.1007/978-3-319-10295-5.
2. Advanced plasma processing technology. New York: John Wiley & Sons Inc. 2008. 479 p.
3. **Wolf S., Tauber R.N.** Silicon Processing for the VLSI Era. Volume 1. Process Technology. New York: Lattice Press. 2000. 416 p.
4. **Donnelly V. M., Kornblit A.** Plasma etching: Yesterday, today, and tomorrow. *J. Vac. Sci. Technol.* 2013. V. 31. P. 050825-48. DOI: 10.1116/1.4819316.

5. **Lieberman M.A., Lichtenberg A.J.** Principles of plasma discharges and materials processing. New York: John Wiley & Sons Inc. 2005. 757 p. DOI: 10.1002/0471724254.
6. **Kemaneci E.H., Carbone E.A.D., Booth J.P., Graef W.A.A.D., Dijk van J., Kroesen G.M.W.** Global (volume-averaged) model of inductively coupled chlorine plasma : influence of Cl wall recombination and external heating on continuous and pulse-modulated plasmas. *Plasma Sources Sci. Technol.* 2014. V. 23(4). P. 045002(1-14). DOI: 10.1088/0963-0252/23/4/045002.
7. **Efremov A., Lee J., Kwon K.-H.** A comparative study of CF_4, Cl_2 and HBr + Ar inductively coupled plasmas for dry etching applications. *Thin Solid Films.* 2017. V. 629. P. 39-48. DOI: 10.1016/j.tsf.2017.03.035.
8. **Malyshev M.V., Donnelly V.M.** Diagnostics of chlorine inductively coupled plasmas. Measurement of electron temperatures and electron energy distribution functions. *J. Appl. Phys.* 2000. V. 87. P. 1642-1650. DOI: 10.1063/1.372072.
9. **Thorsteinsson E.G., Gudmundsson J.T.** A global (volume averaged) model of a chlorine discharge. *Plasma Sources Sci. Technol.* 2010. V. 19. P. 015001 (1-15). DOI: 10.1088/0963-0252/19/1/015001.
10. **Efremov A.M., Kim G.H., Kim J.G., Bogomolov A.V., Kim C.I.** Applicability of self-consistent global model for characterization of inductively coupled Cl_2 plasma. *Vacuum*. 2007. V. 81. N 5. P. 669-675. DOI: 10.1016/j.vacuum.2006.09.017.
11. **Tinck S., Boullart W., Bogaerts A.** Simulation of an Ar/Cl_2 inductively coupled plasma: study of the effect of bias, power and pressure and comparison with experiments. *J. Phys. D. Appl. Phys.* 2008. V. 41. N 18. P. 065207. DOI: 10.1088/0022-3727/41/6/065207.
12. CRC Handbook of Chemistry and Physics. New York: CRC Press. 2010. 2760 p.
13. **Kol S., Oral A.Y.** Hf - based high-k dielectrics: A Review. *Acta Physica Polonica A.* 2019. V. 136(6) P. 873-881. DOI: 10.12693/APhysPolA.136.873.
14. **Clark R.D.** Emerging Applications for High-K Materials in VLSI Technology. *Materials*. 2014. V. 7(4). P. 2913-2944. DOI: 10.3390/ma7042913.
15. **Kim M., Min N.-K., Yun S.J., Lee H.W., Efremov A., Kwon K.-H.** On the etching mechanism of ZrO_2 thin films in inductively coupled BCl_3/Ar plasma. *Microelectronic Eng.* 2008. V. 85(2). P. 348-354. DOI: 10.1016/j.mee.2007.07.009.
16. **Lee C.-I., Kim G.-H., Kim D.-P., Woo J.-C., Kim C.-I.** Dry etching mechanisms of ZrO_2 thin films in BCl_3/Cl_2/Ar plasma. *Ferroelectrics*. 2009. V. 384(1). P. 32-38. DOI: 10.1080/00150190902892725.
17. **Woo J.-C., Yang X., Um D.-S., Kim C.-I.** Dry etching characteristics of ZrO_2 thin films using high density Cl_2/Ar plasma. *Ferroelectrics.* 2010. V. 407(1). P. 117-124. DOI: 10.1080/00150193.2010.484750.
18. **Sha L., Cho B.-O., Chang J. P.** Ion-enhanced chemical etching of ZrO_2 in a chlorine discharge. *J. Vac. Sci. Technol. A.* 2002. V. 20(5). P. 1525-1531. DOI: 10.1116/1.1491267.
19. **Efremov A., Min N.-K., Yun S. J., Kwon K.-H.** Effect of gas mixing ratio on etch behavior of ZrO_2 thin films in Cl_2 - based inductively coupled plasmas. *J. Vac. Sci. Technol. A.* 2008. V. 26(6). P. 1480-1486. DOI: 10.1116/1.2998806.
20. **Efremov A.M., Murin D.B., Betelin V.B., Kwon K.-H.** Special Aspects of the Kinetics of Reactive Ion Etching of SiO_2 in Fluorine-, Chlorine-, and Bromine-Containing Plasma. *Russian Microelectronics.* 2020. V. 49. N 2. P. 94-102. DOI: 10.1134/S1063739720010060.
21. **Shun'ko E.V.** Langmuir probe in theory and practice. Boca Raton: Universal Publ. 2008. 245 p.
22. **Engeln R., Klarenaar B., Guaitella O.** Foundations of optical diagnostics in low-temperature plasmas. *Plasma Sources Sci. Technol.* 2020. V. 29. P. 063001(1-14). DOI: 10.1088/1361-6595/ab6880.
23. **Lopaev D.V., Volynets A.V., Zyryanov S.M., Zotovich A.I., Rakhimov A.T.** Actinometry of O, N and F atoms. *J. Phys. D: Appl. Phys.* 2017. V. 50. P. 075202(1-17). DOI: 10.1088/1361-6463/50/7/075202.
24. **Richards A.D., Thompson B.E., Allen K.D., Sawin H.H.** Atomic chlorine concentration measurements in a plasma etching reactor. I. A comparison of infrared absorption and optical emission actinometry. *J. Appl. Phys.* 1987. V. 62(3). P. 792-279. DOI: 10.1063/1.339734.
25. **Hanish C.K., Grizzle J.W., Teny F.L.** Estimating and controlling atomic chlorine concentration via actinometry. *IEEE Trans. Semicond. Manufact.* 1999. V. 12(3). P. 323-331. DOI: 10.1109/66.778197.
26. **Fuller N., Herman I., Donnelly V.** Optical actinometry of Cl_2, Cl, Cl^+, and Ar^+ densities in inductively coupled Cl_2-Ar plasmas. *J. Appl. Phys.* 2001. V. 90. P. 182-3191. DOI: 10.1063/1.1391222.
27. **Malyshev M.V., Donnelly V.M., Kornblit A., Ciampa N.A.** Percent dissociation of Cl_2 in inductively coupled chlorine-containing plasmas. *J. Appl. Phys.* 1998. V. 84(1). P. 137-146. DOI: 10.1063/1.368010.
28. **Malyshev M.V., Donnelly V.M.,** Diagnostics of inductively coupled chlorine plasmas: Measurement of Cl_2 and Cl number densities. *J. Appl. Phys.* 2000. V. 88(11). P. 6207-6215. DOI: 10.1063/1.1321777.
29. **Hsu C. C., Nierode M. A., Coburn J. W., Graves D. B.** Comparison of model and experiment for Ar, Ar/O_2 and Ar/O_2/Cl_2 inductively coupled plasmas. *J. Phys. D. Appl. Phys*. 2006. V. 39. P. 3272-3284. DOI: 10.1088/0022-3727/39/15/009.
30. **Huang S., Gudmundsson J.** A particle-in-cell/Monte Carlo simulation of a capacitively coupled chlorine discharge. *Plasma Sources Sci. Technol.* 2013. V. 22. P. 055020(1-16). DOI: 10.1088/0963-0252/22/5/055020.
31. **Mione M. A., Katsouras I., Creyghton Y., Boekel W., Maas J., Gelinck G., Roozeboom F., Illiberi A.,** Atmospheric Pressure Plasma Enhanced Spatial ALD of ZrO_2 for Low-Temperature, Large-Area Applications. *J. Solid State Sci. Technol.* 2017. V. 6(12). P. N243-N249. DOI: 10.1149/2.0381712jss.
32. **Efremov A.M., Kim G.H., Kim J.G., Bogomolov A.V., Kim C.I.** On the applicability of self-consistent global model for the characterization of Cl_2/Ar inductively coupled plasma. *Microelectron. Eng.* 2007. V. 84. P.136-143. DOI: 10.1016/j.mee.2006.09.020.
33. **Efremov A.M., Kim D.P., Kim C.I.** Simple model for ion-assisted etching using Cl_2-Ar inductively coupled plasma: Effect of gas mixing ratio. *IEEE Trans. Plasma Sci.* 2004. V. 32. N 3. P. 1344-1351. DOI: 10.1109/TPS.2004.828413.

34. **Meeks E., Ho P., Ting A., Buss R.J.** Simulations of $BCl_3/Cl_2/Ar$ plasmas with comparisons to diagnostic data. *J. Vac. Sci. Technol. A.* 1998. V. 16. P. 2227-2239. DOI: 10.1116/1.581332.
35. **Corr C.S., Despiau-Pujo E., Chabert P., Graham W.G., Marro F.G., Graves D.B.** Comparison between fluid simulations and experiments in inductively coupled argon/chlorine plasmas. *J. Phys. D. Appl. Phys.* 2008. V. 41(18). P. 185-202. DOI: 10.1088/0022-3727/41/18/185202.
36. **Gray D.C., Tepermeister I., Sawin H.H.** Phenomenological modeling of ion enhanced surface kinetics in fluorine-based plasma etching. *J. Vac. Sci. Technol. B.* 1993. V. 11. P. 1243-1257. DOI: 10.1116/1.586925.
37. **Vitale S.A., Chae H., Sawin H. H.** Silicon etching yields in F_2, Cl_2, Br_2, and HBr high density plasmas. *J. Vac. Sci. Technol.* 2001. V. 19. P. 2197-2206. DOI: 10.1116/1.1378077.
38. **Efremov A.M., Smirnov S.A., Betelin V.B., Kwon K.-H.** On the comparison of reactive-ion etching mechanisms for SiO2 in fluorine- and chlorine-containing plasmas. *ChemChemTech [Izv. Vyssh. Uchebn. Zaved. Khim. Khim. Tekhnol.]*. 2023. V. 66. N 8. P. 52-64.
Ефремов А.М., Смирнов С.А., Бетелин В.Б., KwonK.-H. О сравнении механизмов реактивно-ионного травления SiO_2 во фтор-и хлорсодержащей плазме. *Изв. вузов. Химия и хим. технология.* 2023. Т. 66. Вып. 8. С. 54-62. DOI: 10.6060/ivkkt.20236608.6746.
39. **Seah M.P., Nunney T.S.** Sputtering yields of compounds using argon ions. *J. Phys. D: Appl. Phys.* 2010. V. 43 P. 253001 (1-24). DOI: 10.1088/0022-3727/43/25/253001.
40. **Raju G.G.,** Gaseous electronics. Tables, Atoms and Molecules. Boca Raton: CRC Press. 2012. 790 p. DOI: 10.1201/b11492.
41. **Christophorou L.G., Olthoff J.K.** Fundamental electron interactions with plasma processing gases. New York: Springer Science+Business Media LLC. 2004. 776 p. DOI: 10.1007/978-1-4419-8971-0.
42. **Kota G.P., Coburn J.W., Graves D.B.** The recombination of chlorine atoms at surfaces. *J. Vac. Sci. Tech. A.* 1998. V. 16(1). P. 270-277. DOI: 10.1116/1.580982.
43. **Stafford L., Guha J., Khare R., Mattei S., Boudreault O., Clain B., Donnelly V.M.** Experimental and modeling study of O and Cl atoms surface recombination reactions in O_2 and Cl_2 plasmas. *Pure Appl. Chem.* 2010. V. 82(6). P. 1301-1315. DOI: 10.1351/PAC-CON-09-11-02
44. **Efremov A.M., Betelin V.B., Mednikov K.A., Kwon K.-H.** Plasma parameters and densities of active species in mixtures of fluorocarbon gases with argon and oxygen. *ChemChemTech [Izv. Vyssh. Uchebn. Zaved. Khim. Khim. Tekhnol.]*. 2021. V. 64. N 7. P. 46-53.
Ефремов А.М., Бетелин В.Б., Медников К.А., Kwon K.-H. Параметры плазмы и концентрации активных частиц в смесях фторуглеродных газов с аргоном и кислородом. *Изв. вузов. Химия и хим. технология.* 2021. Т. 64. Вып. 7. С. 46-53. DOI: 10.6060/ivkkt.20216407.6390.

Поступила в редакцию 21.02.2024
Принята к опубликованию 08.07.2024

Received 21.02.2024
Accepted 08.07.2024